Temperature-driven tunability of a vanadium dioxide-based microcavity made of random sequences of layers

TRAMAT 1 (2025) 100143

Contents lists available at ScienceDirect

Transactions of Materials Research

journal homepage: www.sciencedirect.com/journal/transactions-of-materials-research

Temperature-driven tunability of a vanadium dioxide-based microcavity made of random sequences of layers

Francesco Scotognella

Department of Applied Science and Technology, Politecnico di Torino, Corso Duca degli Abruzzi 24, Torino, 10129, Italy

ARTICLE INFO

Keywords:
Vanadium dioxide
Microcavities
Phase transition
Tunable optical properties

ABSTRACT

Vanadium dioxide-based photonic devices show significant potential for a range of applications, such as smart windows and reconfigurable optical switches. In this study, we introduce a microcavity design featuring a vanadium dioxide layer positioned between two photonic structures composed of a random sequence of 32 alternating layers of silicon dioxide and zirconium dioxide. The temperature-dependent complex refractive index of vanadium dioxide has been thoroughly accounted for. Our findings reveal that even a temperature change of just 1 °C results in subtle variations in the optical response. These small changes can be detected through differential light transmission measurements, which can be performed using relatively simple and low-cost optical setups. Consequently, the proposed microcavity can serve as an effective temperature sensor or a highly sensitive photon detector, where incident photons induce a temperature rise in the material.

1. Introduction

Crystalline vanadium dioxide (VO_2) undergoes a thermochromic phase transition at approximately 68 °C (341 K) [1,2]. This transition corresponds to a structural shift in the crystal from a monoclinic insulating phase to a tetragonal (rutile) metallic phase [3,4]. Optically, this change transforms VO_2 from a semi-transparent insulator into a more reflective and lossy metallic material [4,5]. The unique characteristics of VO_2 phase transition enable a variety of potential applications, including smart windows, steep-slope devices for microelectronics, neuromorphic computing elements, reconfigurable radiofrequency switches, and THz and mid-infrared absorbers [6–10].

A major effort by the scientific community, responding to a real technological need, is focused on the creation of active photonic devices, and this work is evidenced by numerous reports that can be found in the literature [11–13]. An interesting and simple idea, both from the point of view of modelling the optical response and from the point of view of manufacturing the devices and characterizing them, is to introduce vanadium dioxide between photonic crystals [14–16] in order to create an optical microcavity. The literature on vanadium oxide based photonic crystals is vast. In 2001, Golubev et al. [17] have prepared a silicon dioxide based synthetic opal, i.e., a three-dimensional photonic crystal having a face-centered cubic lattice, they have filled the opal pore with V_2O_5 via chemical bath deposition technique, and they have reduced V_2O_5 to VO_2 by annealing. Golubev et al. have shown that the photonic band gap of such opal-VO_2 composite is governed by the phase transition of vanadium dioxide. In 2002, Golubev et al. [18] have studied in detail the hysteresis of the temperature dependence of the opal-VO_2 composite, in terms of the photonic band gap peak shift and in terms of the electrical conductivity change. In 2008, Ibisate, Golmayo, and López [19] have fabricated VO_2–SiO_2 composite opals and VO_2 inverse opals, demonstrating their thermochromic behavior. In 2010, Pevtsov et al. [20] have fabricated opal-VO_2 composites that show switching, due to the VO_2 transition, of the photonic band gap in the range 1.3–1.6 μm, which is very interesting for telecommunications. In 2019, Wang et al. [21] have demonstrated tunable THz properties of three-dimensional VO_2/PDMS THz photonic crystals. Many interesting works are reported in a review on vanadium dioxide-based tunable photonics by Ko, Badloe, and Rho published in 2021 [11]. More recently, a deep study of the switching in vanadium dioxide-based opals has been reported by Peng et al. [22]. One-dimensional photonic crystals are very useful tools because of their relatively fabrication compatible with many layer-based processing [23]. The combination of a VO_2 layer and a one-dimensional photonic crystal has been studied in several publications [24–29]. Furthermore, Taherzadeh and Keshavarz [30] have proposed vanadium dioxide-based one-dimensional photonic quasicrystal. Finally, it is noteworthy the engineering of vanadium dioxide-based metasurfaces [31–34].

Here, we propose a microcavity in which a vanadium dioxide layer is sandwiched between two photonic structures with a randomized

E-mail address: francesco.scotognella@polito.it.

https://doi.org/10.1016/j.tramat.2025.100143
Received 24 October 2025; Received in revised form 25 November 2025; Accepted 29 November 2025
Available online 3 December 2025

sequence of 32 layers of silicon dioxide layers and zirconium dioxide layers. The temperature-dependent complex refractive index of vanadium dioxide has been carefully considered. While it is particularly apparent that there is a difference in the optical response of the cavity with the vanadium dioxide film all in the insulating phase or all in the metallic phase, it is reported in this work that small differences in the optical response occur even with a temperature change of only 1 °C. This small difference can be measured by a differential measurement of light transmission, a measurement that can be obtained with particularly simple and inexpensive optical apparatus. The distinctive feature of a disordered cavity is that it exhibits a multitude of significantly narrow transmission peaks. With this type of cavity, it is therefore easier to monitor differences in the transmission spectrum and, consequently, to monitor temperature changes. This allows the proposed microcavity to be used as a temperature sensor or photon detector, where photons impacting the microcavity lead to a temperature change in the material.

2. Methods

The complex dielectric function of a vanadium dioxide film can be described with the Looyenga rule [35,36]:

$$\varepsilon_{eff}^{s} = (1-f)\varepsilon_{i}^{s} + f\varepsilon_{m}^{s} \tag{1}$$

In which ε_i is the complex dielectric function of the insulating phase, while ε_m is the complex dielectric function of the metallic phase. The choice of the Looyenga to describe the complex dielectric function of a vanadium dioxide follows the study reported by Wan et al. [36]. In fact, the Looyenga rule can be used to approximate the optical response of vanadium dioxide films within the insulator to metal transition, taking into account the coexistence of insulating and metallic domains. Furthermore, the complex dielectric function is related to the complex refractive index:

$$\varepsilon = n^2 = \left(n_{real} + in_{imag}\right)^2 \tag{2}$$

Where n_{real} is the real part of the complex refractive index, while n_{imag} is the imaginary part of the complex refractive index. The s parameter depends upon the shape of the metallic inclusions in the vanadium dioxide film. Following references [36,37], the value of s in this work is 0.3. Finally, f is the temperature-dependent volume fraction of the vanadium dioxide domains, in the metallic phase, within the film [36]:

$$f(t) = \frac{1}{1 + exp\left[\frac{W}{k_B}\left(\frac{1}{t} - \frac{1}{t_{half}}\right)\right]} \tag{3}$$

In which W is related to the width of the temperature range of the phase transition from insulator to metal of vanadium dioxide, and the parameter t_{half} is the temperature at which half of the film is in the metallic phase. k_B is the Boltzmann constant in eV/K (i.e., $k_B = 8.617 \times 10^{-5}\ eV/K$). t_{half} is taken from Ref. [36], and its value is 78.5 °C. The temperatures in Equation (3) are in Kelvin. For a deeper understanding of these parameters we invite the reader to read the comprehensive discussion of Ref. [36].

The wavelength dependent refractive index $n_k(\lambda)$ of silicon dioxide (zirconium dioxide) can be written with the Sellmeier equation

$$n_{SiO_2(ZrO_2)}^2(\lambda) - 1 = \sum_{j=1,2,3} \frac{A_j\lambda^2}{\lambda^2 - B_j^2} \tag{4}$$

The parameters A_j and B_j for the two different oxides are reported in Table 1.

The optical response, in terms of light transmission, of the microcavity in the spectral range between 300 nm and 2000 nm has been studied with the transfer matrix method [41–43]. The system is glass/-microcavity/air, and the light is impinging orthogonally the surface of the sample. The characteristic matrix of the multilayered microcavity is written as

$$M = \begin{bmatrix} M_{11} & M_{12} \\ M_{21} & M_{22} \end{bmatrix} = \prod_{k=1}^{N} \begin{bmatrix} cos\left(\frac{2\pi}{\lambda} n_k(\lambda) d_k\right) & -\frac{i}{n_k(\lambda)} sin\left(\frac{2\pi}{\lambda} n_k(\lambda) d_k\right) \\ -in_k(\lambda) sin\left(\frac{2\pi}{\lambda} n_k(\lambda) d_k\right) & cos\left(\frac{2\pi}{\lambda} n_k(\lambda) d_k\right) \end{bmatrix} \tag{5}$$

where $k = (1, \ldots, N)$ and N represents the number of layers. The parameters d_k and $n_k(\lambda)$ are, respectively, the thickness and the wavelength dependent refractive index of the kth layer. The light transmitted by the sample is written as

$$T = \frac{n_0}{n_g} \left| \frac{2n_g}{(M_{11} + M_{12}n_0)n_g + (M_{21} + M_{22}n_0)} \right|^2 \tag{6}$$

with n_g the refractive index of glass (we have employed Equation (4) considering a glass made of silicon dioxide) and n_0 the refractive index of air ($n_0 \cong 1$). The light transmission has been calculated between 300 nm and 2000 nm with steps of 0.25 nm.

3. Results and discussion

The microcavity has been engineering sandwiching a layer of vanadium dioxide between two photonic structures with a randomized sequence of silicon dioxide and zirconium dioxide layers. A sketch of the microcavity is depicted in Fig. 1a.

In such photonic structures of 32 layers each, the thickness of the silicon dioxide layers is 220 nm, the thickness of the zirconium dioxide layers is 165 nm. The thickness of the vanadium dioxide layer in the microcavity is 55 nm. The thicknesses of the silicon dioxide layers and zirconium dioxide layer are chosen since a corresponding periodic photonic crystal made of silicon dioxide and zirconium dioxide leads to a photonic band gap between 1000 nm and 1500 nm. The thickness of 55 nm for vanadium dioxide allows us to obtain a reasonably low absorption by the material. The random sequence has been generated by employing an algorithm that generates uniformly distributed random integers between 1 and 2, assigning the layers of silicon dioxide to 1 and the layers of zirconium dioxide to 2. The sequence of layers in the microcavity is ZZSZZSSZZZSZZZZSZSZZZZZSZSZSSSSZVZSZSSZZZ ZSZZZSZSZSZSSSZZSSSZZZSZ (with Z zirconium dioxide, S silicon dioxide, V vanadium dioxide).

In Fig. 1b we show the transmission spectra, at 60 °C and at 100 °C, of the microcavity in which a vanadium dioxide layer is sandwiched between two photonic structures made by a random sequence of silicon dioxide and zirconium dioxide layers. It is evident that, because of the different refractive indexes of the insulating phase and the metallic phase of vanadium dioxide, several transmission peaks in the range between 300 nm and 2000 nm are remarkably changing.

In Fig. 2 a contour plot, which describes the dependence upon wavelength and temperature of the studied microcavity, is depicted in the spectral range between 1250 nm and 1500 nm. This graph shows

Table 1
Parameters of the Sellmeier equation for SiO_2 and ZrO_2.

Material	A_1	B_1	A_2	B_2	A_3	B_3	Ref.
SiO_2	0.6961663	0.0684043	0.4079426	0.1162414	0.8974794	9.896161	[38,39]
ZrO_2	1.347091	0.062543	2.117788	0.166739	9.452943	24.32057	[40]

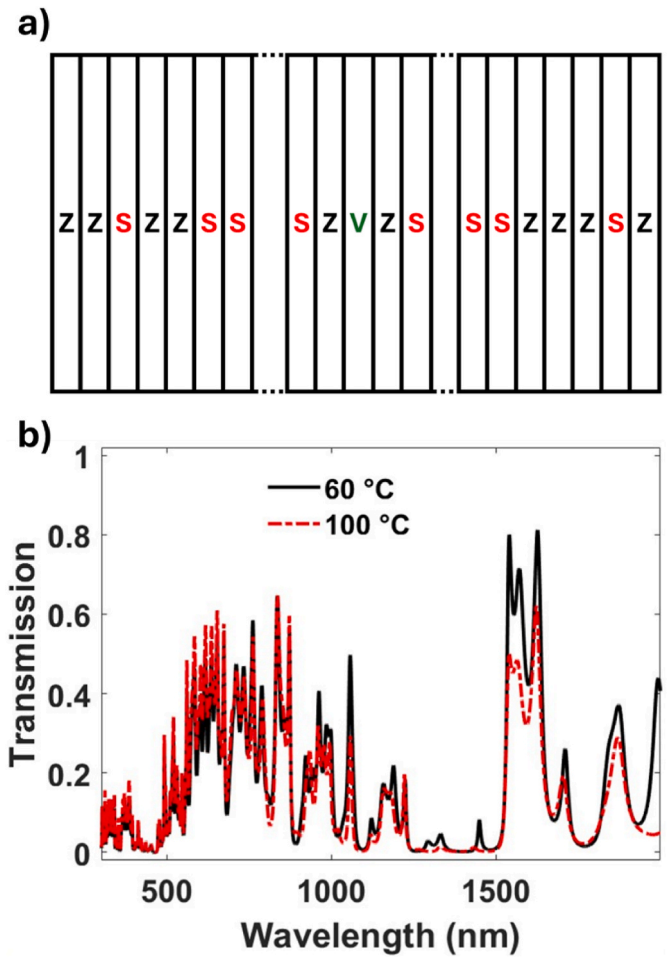

Fig. 1. (a) sketch of the disordered microcavity, in which Z, S, and V indicate zirconium dioxide, silicon dioxide, and vanadium dioxide, respectively. (b) Transmission spectra at 60 °C and 100 °C of the microcavity in which a vanadium dioxide layer is sandwiched between two photonic structures made by a random sequence of silicon dioxide and zirconium dioxide layers.

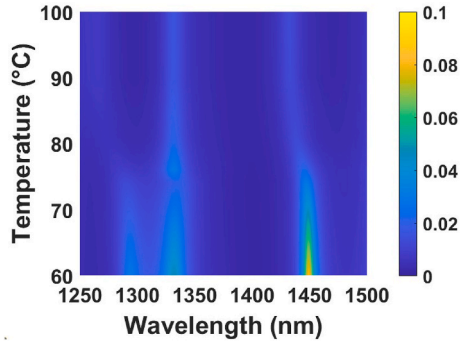

Fig. 2. Transmission of the random SiO2/ZrO2 cavity hat embed a VO2 layer as a function of wavelength and temperature.

that the most significant changes in the transmission spectrum of the microcavity occur at the phase transition of vanadium dioxide.

Fig. 3 (top) shows the transmission spectra at 77 °C and 78 °C of a microcavity in which a vanadium dioxide layer is sandwiched between two photonic structures made by a random sequence of silicon dioxide and zirconium dioxide layers, in the range 1100–1500 nm. Instead, Fig. 3 (bottom) shows the differential transmission $\Delta T/T = (T_{t=78\,^\circ C} - T_{t=77\,^\circ C})/T_{t=77\,^\circ C}$. A measurement of the differential

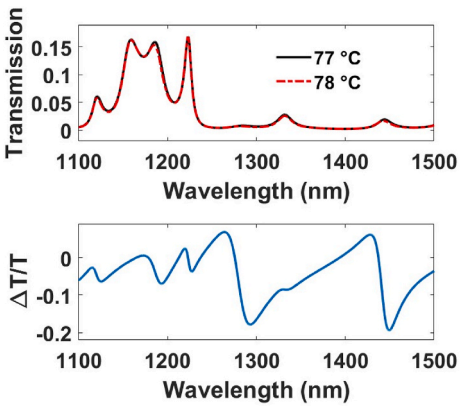

Fig. 3. (top) Transmission spectra at 77 °C and 78 °C of a microcavity in which a vanadium dioxide layer is sandwiched between two photonic structures made by a random sequence of silicon dioxide and zirconium dioxide layers, in the range 1100–1500 nm. (bottom) Differential transmission $\Delta T/T = (T_{t=78\,^\circ C} - T_{t=77\,^\circ C})/T_{t=77\,^\circ C}$.

transmission can be performed with different setups as in Ref. [44]. The mean value of the $\Delta T/T$ (absolute value) in the region 1100–1500 nm is 0.0584, while the standard deviation of the absolute value of $\Delta T/T$ in the region mentioned above is 0.0477. It is noteworthy to see a transmission decrease of almost 20 % at around 1450 nm with a temperature increase of a degree. Such difference is due to the significant variations in the real and imaginary parts of the refractive index of vanadium because of the change of temperature. In fact, by increasing the temperature, at 1450 nm the real part of the refractive index of vanadium dioxide is decreasing, while its imaginary part is increasing [36]. In Table 2 the position in the spectrum and the full width at half maximum (FWHM) of the transmission peak around 1450 nm are reported for the aforementioned temperatures, i.e., 77 °C and 78 °C. By increasing the temperature, together with the blue shift of the transmission peak, a slight peak broadening is remarkable.

In Figure A2 of the appendix, a microcavity in which an uncertainty of 4 nm (following a uniform distribution) in each layer thickness has been considered, in order to simulate an experimental uncertainty in the deposition of each layer. It is evident that, also with this uncertainty, the difference in the spectra at 77 °C and at 78 °C can be detected.

In Figure A3 of the appendix, the angular dependence of the transmission spectrum at 77 °C of the vanadium dioxide-based microcavity has been reported. The simulation has been performed for transverse electric (TE) and transverse magnetic (TM) waves. A more in-depth study of the interrelationship between the optical response as a function of temperature and the optical response as a function of the angle of incidence of light is suggested for future work.

For a better comprehension of the physical mechanisms in the vanadium dioxide-based disordered microcavity, we have simulated the electric field distribution along the microcavity sample, following the methodology described in Wiersma et al. [45]. In Fig. 4a (top) we have reported a contour plot related to the light transmission along the sample at 78 °C, with the sample length in the x-axis and the wavelength in the y-axis. In Fig. 4a (bottom) we have reported the contour plot corresponding to the electric field, in logarithmic scale, along the sample at 78 °C. Finally, in Fig. 4b we have displayed the electric field, related to the wavelength of 1450 nm, along the sample at 77 °C (black solid

Table 2
Position and full width at half maximum (FWHM) of the transmission peak around 1450 nm at 77 °C and 78 °C.

Temperature (°C)	Transmission peak position (nm)	FWHM (nm)
77	1444.25	20.5
78	1442.75	22.75

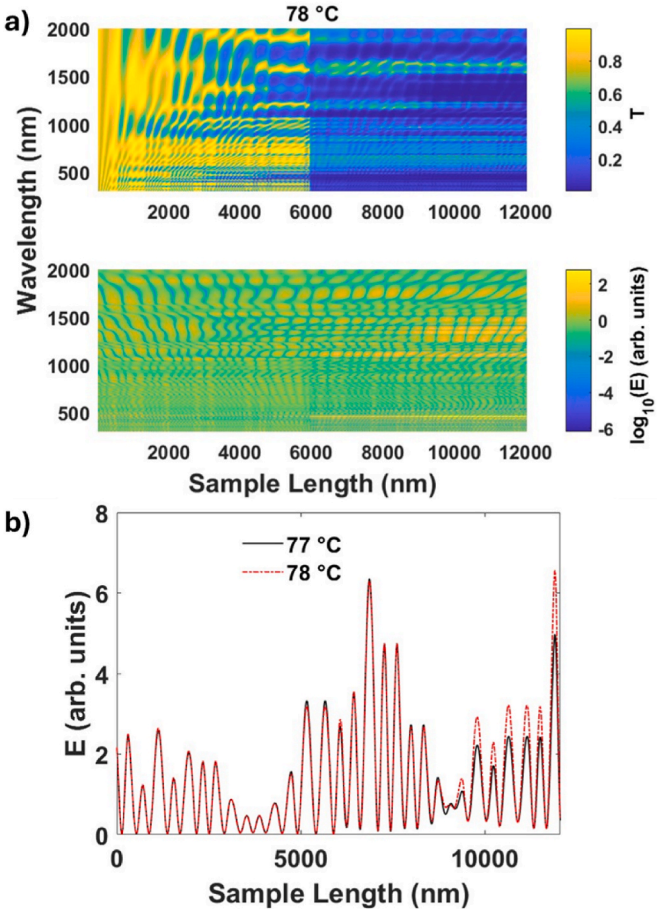

Fig. 4. (a, top) Contour plot of the light transmission along the sample at 78 °C, with the sample length in the x-axis and the wavelength in the y-axis; (a, bottom) Contour plot of the electric field, in logarithmic scale, along the sample at 78 °C. (b) Electric field, related the wavelength of 1450 nm, along the sample at 77 °C (black solid curve) and at 78 °C (red dashed curve).

curve) and at 78 °C (red dashed curve). We can observe that transmission is dramatically reduced in the middle of the sample, where the defect made of vanadium dioxide is placed, and this is due to the imaginary part of the refractive index of vanadium dioxide that is related to a light absorption contribution.

After the vanadium dioxide defect, in such microcavity we have observed stronger electric field peaks, and this could be ascribed to the possibility of local mode enhancements. However, a better understanding of the physical phenomenon and more investigations are necessary, and this could be the subject of future studies. Focusing at 1450 nm, we have observed that the electric field, after the vanadium dioxide defect, shows more intense peaks by increasing the temperature from 77 °C to 78 °C.

4. Conclusion

In this study, we modeled a microcavity incorporating a vanadium dioxide layer positioned between two photonic structures composed of a random sequence of 32 alternating silicon dioxide and zirconium dioxide layers. The complex refractive index of vanadium dioxide was rigorously considered, accounting for both its wavelength and temperature dependencies. While the distinct optical responses of the cavity with vanadium dioxide in its insulating and metallic phases are clearly pronounced, our findings demonstrate that even a temperature variation as small as 1 °C induces subtle yet measurable changes in the optical response. These minor variations can be detected using differential light transmission measurements, which can be performed with relatively simple and cost-effective optical instrumentation. One notable thing is that the relationship between refractive index and temperature is different when the sample is heated or cooled [36]. In this work, we limited ourselves to the case of heating. The studied vanadium oxide-based random microcavity can be employed as a temperature sensor. Alternately, the microcavity can be used as a photon detector, because photons striking such microcavity cause a temperature change in the material.

Declaration of competing interest

The authors declare that they have no known competing financial interests or personal relationships that could have appeared to influence the work reported in this paper.

Acknowledgement

This project has received funding from the European Research Council (ERC) under the European Union's Horizon 2020 research and innovation programme (grant agreement No. [816313]) and the EIC LEAF (grant agreement No. [101186701]). The project has received funding from PRIN 2022ZMA4X3 – ERACLITO.

Appendix

In Figure A1 the transmission spectra at 60 °C of the vanadium dioxide-based random photonic structures for five different permutations of the random sequence of silicon dioxide and zirconium dioxide layers are shown. It is evident that each permutation leads to a completely different transmission spectrum.

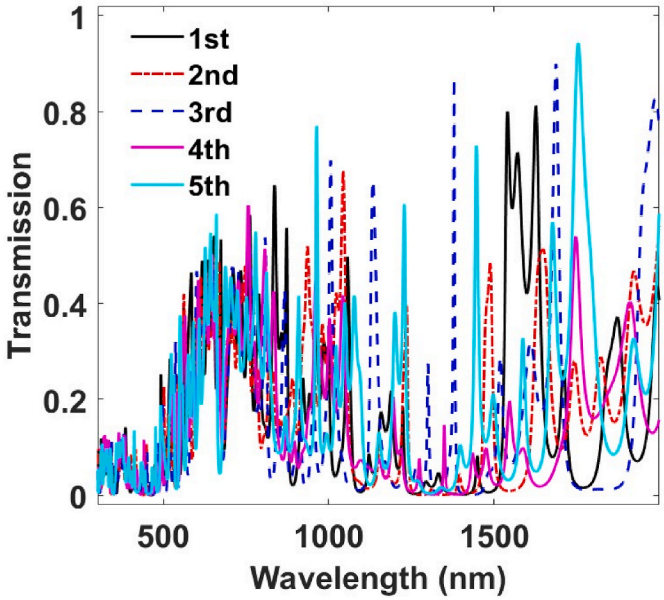

Fig. A1. Transmission spectra at 60 °C of the vanadium dioxide-based random photonic structures for five different permutations of the random sequence of silicon dioxide and zirconium dioxide layers.

In Figure A2 there are shown the transmission spectra at 77 °C and 78 °C, in the range 1100–1500 nm, of the vanadium dioxide-based microcavity with an uncertainty of 4 nm for each layer thickness (e.g., the thickness of silicon dioxide layers is 220 ± 2 nm).

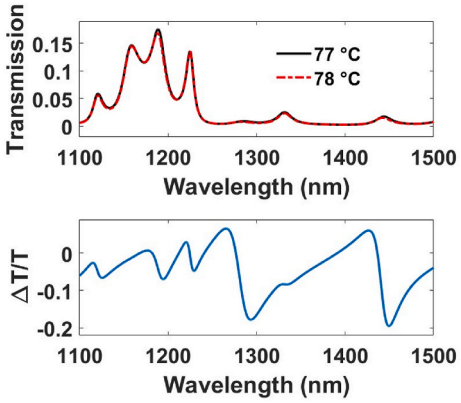

Fig. A2. Transmission spectra at 77 °C and 78 °C, in the range 1100–1500 nm, of the vanadium dioxide-based microcavity with an uncertainty of 4 nm for each layer thickness.

In Figure A3 the angular dependence of the transmission spectrum at 77 °C of the vanadium dioxide-based microcavity is shown. Figure A3 top shows the transverse electric (TE) waves, while figure A3 bottom shows the transverse magnetic (TM) waves. The method followed is described in Ref. [46].

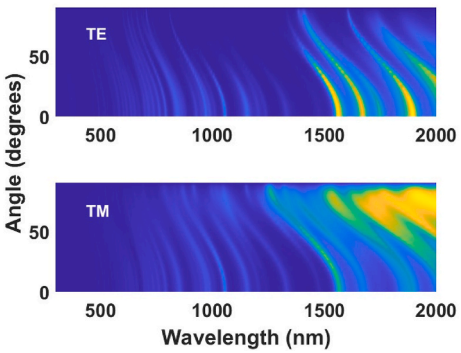

Fig. A3. Angular dependence of the transmission spectrum at 77 °C of the vanadium dioxide-based microcavity. Top: transverse electric (TE) waves; bottom: transverse magnetic (TM) waves.

References

[1] F.J. Morin, Oxides which show a metal-to-insulator transition at the neel temperature, Phys. Rev. Lett. 3 (1959) 34–36, https://doi.org/10.1103/PhysRevLett.3.34.

[2] J.-P. Pouget, Basic aspects of the metal–insulator transition in vanadium dioxide VO 2 : a critical review, C. R. Phys. 22 (2021) 37–87, https://doi.org/10.5802/crphys.74.

[3] R.M. Briggs, I.M. Pryce, H.A. Atwater, Compact silicon photonic waveguide modulator based on the vanadium dioxide metal-insulator phase transition, Opt. Express 18 (2010) 11192–11201, https://doi.org/10.1364/OE.18.011192.

[4] M. Currie, M.A. Mastro, V.D. Wheeler, Characterizing the tunable refractive index of vanadium dioxide, Opt. Mater. Express 7 (2017) 1697–1707, https://doi.org/10.1364/OME.7.001697.

[5] H.W. Verleur, A.S. Barker, C.N. Berglund, Optical Properties of V${\mathrm{O}}_{2}$ between 0.25 and 5 eV, Phys. Rev. 172 (1968) 788–798, https://doi.org/10.1103/PhysRev.172.788.

[6] K. Liu, S. Lee, S. Yang, O. Delaire, J. Wu, Recent progresses on physics and applications of vanadium dioxide, Mater. Today 21 (2018) 875–896, https://doi.org/10.1016/j.mattod.2018.03.029.

[7] H. Lu, S. Clark, Y. Guo, J. Robertson, The metal–insulator phase change in vanadium dioxide and its applications, J. Appl. Phys. 129 (2021) 240902, https://doi.org/10.1063/5.0027674.

[8] M. Darwish, Y. Zhabura, L. Pohl, Recent advances of VO2 in sensors and actuators, Nanomaterials 14 (2024) 582, https://doi.org/10.3390/nano14070582.

[9] J. Wang, M. Liu, H. Yang, Z. Yi, C. Tang, F. Gao, J. Wang, B. Li, Tunable mid-infrared ultra-wideband absorption device with annular-square open metamaterials based on VO2 phase change, Micro Nanostruct. 208 (2025) 208353, https://doi.org/10.1016/j.micrna.2025.208353.

[10] H. Wang, Z. Yi, S. Cheng, C. Tang, F. Gao, B. Li, Graphene-synergized vanadium dioxide phase transition-based terahertz wideband intelligent temperature-controlled absorber, Infrared Phys. Technol. 152 (2025) 106218, https://doi.org/10.1016/j.infrared.2025.106218.

[11] B. Ko, T. Badloe, J. Rho, Vanadium dioxide for dynamically tunable photonics, ChemNanoMat 7 (2021) 713–727, https://doi.org/10.1002/cnma.202100060.

[12] S. Li, X. Liu, S. Zong, J. Chen, G. Liu, J. Chen, C. Tang, Z. Liu, Direction-switchable self-thermophoresis motor with chiral antihelical Resonators, ACS Photonics 11 (2024) 3822–3828, https://doi.org/10.1021/acsphotonics.4c01126.

[13] S. Li, Z. Wu, X. Liu, Q. Ye, G. Liu, J. Chen, W. Du, C. Tang, Z. Liu, Monochromatic Polarization-sensitive photothermoelectric detection via plasmonic quasi-BICs, Laser Photon. Rev. 19 (2025) e00477, https://doi.org/10.1002/lpor.202500477.

[14] S. John, Strong localization of photons in certain disordered dielectric superlattices, Phys. Rev. Lett. 58 (1987) 2486–2489, https://doi.org/10.1103/PhysRevLett.58.2486.

[15] E. Yablonovitch, Inhibited spontaneous emission in solid-state physics and electronics, Phys. Rev. Lett. 58 (1987) 2059–2062, https://doi.org/10.1103/PhysRevLett.58.2059.

[16] J.D. Joannopoulos (Ed.), Photonic Crystals: Molding the Flow of Light, second ed., Princeton University Press, Princeton, 2008.

[17] V.G. Golubev, VYu Davydov, N.F. Kartenko, D.A. Kurdyukov, A.V. Medvedev, A. B. Pevtsov, A.V. Scherbakov, E.B. Shadrin, Phase transition-governed opal–VO2 photonic crystal, Appl. Phys. Lett. 79 (2001) 2127–2129, https://doi.org/10.1063/1.1406144.

[18] V.G. Golubev, D.A. Kurdyukov, A.B. Pevtsov, A.V. Sel'kin, E.B. Shadrin, A. V. Il'inskii, R. Boeyink, Hysteresis of the photonic band gap in VO2 photonic crystal in the semiconductor-metal phase transition, Semiconductors 36 (2002) 1043–1047, https://doi.org/10.1134/1.1507288.

[19] M. Ibisate, D. Golmayo, C. López, Vanadium dioxide thermochromic opals grown by chemical vapour deposition, J. Opt. Pure Appl. Opt. 10 (2008) 125202, https://doi.org/10.1088/1464-4258/10/12/125202.

[20] A.B. Pevtsov, S.A. Grudinkin, A.N. Poddubny, S.F. Kaplan, D.A. Kurdyukov, V. G. Golubev, Switching of the photonic band gap in three-dimensional film photonic crystals based on opal-VO2 composites in the 1.3–1.6 μm spectral range, Semiconductors 44 (2010) 1537–1542, https://doi.org/10.1134/S1063782610120018.

[21] R. Wang, W. Yang, S. Gao, X. Ju, P. Zhu, B. Li, Q. Li, Direct-writing of vanadium dioxide/polydimethylsiloxane three-dimensional photonic crystals with thermally tunable terahertz properties, J. Mater. Chem. C 7 (2019) 8185–8191, https://doi.org/10.1039/C8TC05759A.

[22] J. Peng, J. Brandt, M. Pfeiffer, L. G. Maragno, T. Krekeler, N. T. James, J. Henf, C. Heyn, M. Ritter, M. Eich, et al., Switchable 3D photonic crystals based on the insulator-to-metal transition in VO2, ACS Appl. Mater. Interfaces 16 (2024) 67106–67115, https://doi.org/10.1021/acsami.4c13789.

[23] P. Lova, G. Manfredi, D. Comoretto, Advances in functional solution processed planar 1D photonic crystals, Adv. Opt. Mater. 6 (2018) 1800730, https://doi.org/10.1002/adom.201800730.

[24] A. Rashidi, A. Hatef, A. Namdar, On the enhancement of light absorption in vanadium dioxide/1D photonic crystal composite nanostructures, J. Phys. Appl. Phys. 51 (2018) 375102, https://doi.org/10.1088/1361-6463/aad70a.

[25] D.U. Singh, O. Bhoite, R. Narayanan, Temperature tunable optical transmission using IR based 1D photonic crystals of VO$\less$sub$\greater$2$\less$/sub$\greater$ nanostructures, J. Phys. Appl. Phys. 53 (2020) 245106, https://doi.org/10.1088/1361-6463/ab7d69.

[26] J. Kui Zhang, J. Ming Shi, M. Li, B. Liu, Simulation and preparation of hybrid one dimensional photonic crystal containing phase transition vanadium dioxide, Opt. Mater. 109 (2020) 110275, https://doi.org/10.1016/j.optmat.2020.110275.

[27] F. Scotognella, Vanadium oxide metal-insulator phase transition in different types of one-dimensional photonic microcavities, Front Photon. (2023) 4, https://doi.org/10.3389/fphot.2023.1081521.

[28] B. Roumi, R. Abdi-Ghaleh, H. Akkus, Single-frequency into dual-frequency absorption switch based on a one-dimensional photonic crystal containing graphene and vanadium dioxide layers, Photon. Nanostruct: Fundam. Appl. 53 (2023) 101111, https://doi.org/10.1016/j.photonics.2023.101111.

[29] Z. Ai, H. Yang, M. Liu, S. Cheng, J. Wang, C. Tang, F. Gao, B. Li, Phase-transition-enabled dual-band camouflage in VO2/Ag multilayered nanostructures, Phys. E Low-Dimens. Syst. Nanostruct. 173 (2025) 116327, https://doi.org/10.1016/j.physe.2025.116327.

[30] S. Taherzadeh, A. Keshavarz, Optical bistability in vanadium dioxide photonic crystals engineered with one-dimensional fibonacci sequences, Phys. Wave Phenom. 32 (2024) 401–409, https://doi.org/10.3103/S1541308X24700407.

[31] K. Sun, W. Xiao, C. Wheeler, M. Simeoni, A. Urbani, M. Gaspari, S. Mengali, CH (Kees) de Groot, O.L. Muskens, VO2 metasurface smart thermal emitter with high visual transparency for passive radiative cooling regulation in space and terrestrial applications, Nanophotonics 11 (2022) 4101–4114, https://doi.org/10.1515/nanoph-2022-0020.

[32] B. Li, R. Camacho-Morales, N. Li, A. Tognazzi, M. Gandolfi, D de Ceglia, C. D. Angelis, A.A. Sukhorukov, D.N. Neshev, Fundamental limits for transmission modulation in VO_2 metasurfaces, Photonics Res. 11 (2023) B40–B49, https://doi.org/10.1364/PRJ.474328.

[33] A. Tognazzi, M. Gandolfi, B. Li, G. Ambrosio, P. Franceschini, R. Camacho-Morales, A.C. Cino, C. Baratto, D de Ceglia, D. Neshev, et al., Opto-thermal dynamics of thin-film optical limiters based on the VO_2 phase transition, Opt. Mater. Express 13 (2023) 41–52, https://doi.org/10.1364/OME.472347.

[34] T. Xu, W. Zhang, Q. Song, Z. Yi, C. Ma, S. Cheng, Z. Hao, T. Sun, P. Wu, C. Tang, et al., Thermotunable mid-infrared metamaterial absorption material based on combined hollow cylindrical VO2 structure, Surf. Interfaces 52 (2024) 104868, https://doi.org/10.1016/j.surfin.2024.104868.

[35] H. Looyenga, Dielectric constants of heterogeneous mixtures, Physica 31 (1965) 401–406, https://doi.org/10.1016/0031-8914(65)90045-5.

[36] C. Wan, Z. Zhang, D. Woolf, C.M. Hessel, J. Rensberg, J.M. Hensley, Y. Xiao, A. Shahsafi, J. Salman, S. Richter, et al., On the optical properties of thin-film vanadium dioxide from the visible to the far infrared, Ann. Phys. (Oxford, U. K.) 531 (2019) 1900188, https://doi.org/10.1002/andp.201900188.

[37] J. Rensberg, S. Zhang, Y. Zhou, A.S. McLeod, C. Schwarz, M. Goldflam, M. Liu, J. Kerbusch, R. Nawrodt, S. Ramanathan, et al., Active optical metasurfaces based on defect-engineered phase-transition materials, Nano Lett. 16 (2016) 1050–1055, https://doi.org/10.1021/acs.nanolett.5b04122.

[38] I.H. Malitson, Interspecimen comparison of the refractive index of fused silica, JOSA 55 (1965) 1205–1209, https://doi.org/10.1364/JOSA.55.001205.

[39] C.Z. Tan, Determination of refractive index of silica glass for infrared wavelengths by IR spectroscopy, J. Non-Cryst. Solids 223 (1998) 158–163, https://doi.org/10.1016/S0022-3093(97)00438-9.

[40] D.L. Wood, K. Nassau, Refractive index of cubic zirconia stabilized with yttria, Appl. Opt. 21 (1982) 2978–2981, https://doi.org/10.1364/AO.21.002978.

[41] M. Born, E. Wolf, A.B. Bhatia, P.C. Clemmow, D. Gabor, A.R. Stokes, A.M. Taylor, P.A. Wayman, W.L. Wilcock, Principles of Optics: Electromagnetic Theory of Propagation, Interference and Diffraction of Light, seventh ed., Cambridge University Press, 1999 https://doi.org/10.1017/CBO9781139644181.

[42] X. Xiao, W. Wenjun, L. Shuhong, Z. Wanquan, Z. Dong, D. Qianqian, G. Xuexi, Z. Bingyuan, Investigation of defect modes with Al2O3 and TiO2 in one-dimensional photonic crystals, Optik 127 (2016) 135–138, https://doi.org/10.1016/j.ijleo.2015.10.005.

[43] G.M. Paternò, L. Moscardi, S. Donini, D. Ariodanti, I. Kriegel, M. Zani, E. Parisini, F. Scotognella, G. Lanzani, Hybrid one-dimensional plasmonic–photonic crystals for optical detection of bacterial contaminants, J. Phys. Chem. Lett. 10 (2019) 4980–4986, https://doi.org/10.1021/acs.jpclett.9b01612.

[44] Wohlgenannt M, Ehrenfreund E, Vardeny ZV. "Spectroscopy of long-lived photoexcitations in π-conjugated systems," in Photophysics of Molecular Materials, ed. G. Lanzani (Wiley), 183–259. doi:10.1002/3527607323.ch5.

[45] D.S. Wiersma, R. Sapienza, S. Mujumdar, M. Colocci, M. Ghulinyan, L. Pavesi, Optics of nanostructured dielectrics, J. Opt. Pure Appl. Opt. 7 (2005) S190, https://doi.org/10.1088/1464-4258/7/2/025.

[46] S.K. Awasthi, U. Malaviya, S.P. Ojha, N.K. Mishra, B. Singh, Design of a tunable polarizer using a one–dimensional nano sized photonic bandgap structure, Prog. Electromagn. Res. B 5 (2008) 133–152, https://doi.org/10.2528/PIERB08021004.